URSI GASS 2020, Rome, Italy, 29 August - 5 September 2020

The Physical Perspective of Correlated SAR Clutter

Dong-Xiao Yue, Feng Xu*
Key Lab for Information Science of Electromagnetic Waves (MoE), Fudan University, Shanghai 200433, China, e-mail: fengxu@fudan.edu.cn

Abstract

The development of SAR technology brings a large number of high-resolution SAR images. SAR clutter in these images contains rich environmental information which is inappropriate to be modeled by a single simple statistical model as traditional approaches. It is very critical to reveal the physical information stored in these images for further interpretation and applications of SAR images. This paper aims to give a physical perspective of the correlated SAR clutter starting from the coherent scatterer model. The Gaussian coherent scatterer (GGCS) model kicks off the first step in modeling the physical processes of clutter and the probabilistic graphical network is expected to be an effective intelligent realization of the GGCS model.

1 Introduction

As the development of the high-resolution synthetic aperture radar (SAR), a large number of high-resolution SAR images are obtained which are urgently needed for in-depth analysis. The statistical representation of SAR clutter is a fundamental research for further interpretation and applications of SAR images such as despeckling, target detection and recognition [1,2].

Traditional statistical methods are usually based on the distributional characteristics of pixel values and their relationships. They only consider the high-level cognitive characteristics of the image, but do not necessary take into account the actual scattering and imaging mechanism [1,3]. As the improvement of the resolution of SAR images, the limitations of such approaches show up gradually due to the lack of physical information. In recent years, the research on high-resolution SAR image statistical modeling has refocused on the physical process of electromagnetic scattering [4-6]. As a consequence, the early non-Rayleigh speckle model based on scattering process modeling reclaims a prominent position [1,7]. It is developed based on the coherent scatterer model which models the SAR clutter as the coherent sum of a large number of complex-valued components with independent phases. Many existing distributions can be obtained as some special case under the coherent scatterer model from the perspective of scattering process [6]. It shows that the statistical characteristics of SAR clutter is determined by the statistical setting of the scattered field of a single scatterer and the number of scatterers in a resolution cell. Besides, the traditional statistical methods usually ignore the spatial correlation which brings the texture information of SAR clutter. It is therefore very critical to describe the correlation characteristic of the physical scene. This physical analysis inspires the proposal of the generalized Gaussian coherent scatterer (GGCS) model.

The GGCS model can be seen as a simplification of the coherent scatterer model which assumes the underlying scatterers are Gaussian distributed [6]. It is physics-plausible and can be used to simulate correlated SAR clutter of various scenarios. Most existing single-point distributions can be seen as a special case of the GGCS model by stipulating the distribution of the number of scatterers in each pixel. The rich representation capability and physical interpretability of the GGCS model show its potential in the future applications. However, an intelligent realization for parameter estimation and automated physical analysis of GGCS are still remained to be solved. Aiming at these two problems, an efficient learning framework is undoubtedly needed. The main characteristics of GGCS realization are randomness and convolutional realization. These two points inspire us to model a probabilistic graphical network which represents the GGCS model by a multi-layer probabilistic convolutional neural network [8].

In this paper, the physical analysis of non-Rayleigh speckle model based on the coherent scatterer model is given in Section 2. Section 3 describes the GGCS model and the probabilistic graphical network framework is given in Section 4. Section 5 comes to conclusion.

2 Physical analysis based on the coherent scatterer model

The coherent scatterer model, also known as the discrete scatterer model, describes the speckle phenomenon caused by the coherent sum of complex-valued scattered field of scatterers in a resolution cell. Such a model describes the complex return from a single-image cell as

$$\begin{aligned} \boldsymbol{A} = Ae^{j\phi} = \Re + j\Im = \sum_{i=1}^{N} \boldsymbol{a}_i = \sum_{i=1}^{N} a_i e^{j\phi_i} \\ = \sum_{i=1}^{N} (\Re_i + j\Im_i), \end{aligned} \tag{1}$$

where $\boldsymbol{A}$ is the amplitude of the received signal, ϕ its phase, $j=\sqrt{-1}$, and $\Re$ and $\Im$ the decomposition of $\boldsymbol{A}$ in its real and imaginary parts. These components are the coherent sum of the electromagnetic scattered fields from N independent scatterers, each with amplitude a_i and phase ϕ_i. Equation (1) shows that the statistical properties of the scattered field $\boldsymbol{A}$ are completely determined by the statistical properties of $\{a_i, \phi_i, N\}$ or $\{\Re_i, \Im_i, N\}$. And the following assumptions are adopted [1,6]:

1) a_i, a_j, ϕ_i, ϕ_j, $(i \neq j)$ are collectively independent random variables;
2) $\{\phi_i\}$ is uniformly distributed at $[0,2\pi)$.

Based on the coherent scatterer model, many non-Rayleigh statistical distributions can be summarized by starting from the modeling of the number of scatterers and the amplitude of the scatterers as shown in Figure 1. The number of scatterers in a single resolution cell can typically be modeled as a constant (including infinite constant and finite constant) or a variable obeying a certain distribution (such as the Poisson and negative binomial distributions). The scattered amplitude of each scatterer can be modeled as 1) a constant, 2) a number of independent identically distributed variables (such as K distribution, Rayleigh distribution, or arbitrary distribution), and 3) sum of a constant and an infinite number of variables.

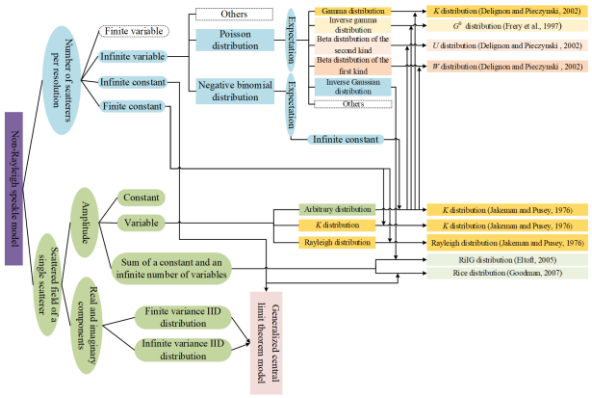

Figure 1. Physical analysis of the intensity distributions based on non-Rayleigh speckle model

If the number of scatterers is an infinite constant and the scattered amplitude is modeled as the sum of a known constant and an infinite number of independent identically distributed (IID) variables, then the Rice (or Rician) distributed scattered field can be obtained [9]. Rician inverse Gaussian (RiIG) distributed intensity can be obtained by mixing the Rician distribution and inverse Gaussian distribution which is explained by Brownian motion with a stop time [10]. Interestingly, RiIG distribution can also be explained using the non-Rayleigh speckle model. If the number of scatterers is modeled as Poisson distribution with its expectation obeying inverse Gaussian distribution and the amplitude is modeled as the sum of a known constant and an infinite number of IID variables, then RiIG distributed intensity is obtained [10]. If the number of scatterers is modeled as a Poisson distribution, and the expectation of the Poisson distribution is also a random variable which can be modeled as gamma distribution, inverse gamma distribution, Beta distribution of the second kind, and Beta distribution of the first kind, then the scattered intensity obeying K distribution, G^0 distribution, U distribution and W distribution can be respectively obtained by combing the above different distributions of Poisson expectation and amplitude with arbitrary distribution [11-13].

3 GGCS model

The physical analysis for non-Rayleigh distributions reveals the interpretation ability of the coherent scatterer model. The GGCS model [6] is a simplification of the coherent scatterer model, which assumes that the pair $(\Re_i, \Im_i)$ obeys an α-stable law, of which the Gaussian distribution is a special case. Figure 2 describes the GGCS model where r and c denote the range and azimuth dimensions of a 2-D region. The black spots represent individual scatterers with a complex-valued scattered field of $\boldsymbol{a}_{r,c}$:

$$\boldsymbol{a}_{r,c} = \Re_{r,c} + j\Im_{r,c}, \tag{2}$$

where $\Re_{r,c}$ and $\Im_{r,c}$ represent, respectively, the real and imaginary components, and both are Gaussian random variables with mean μ and variance σ^2

$$\begin{aligned} \Re_{r,c} &\sim N(\mu, \sigma^2) \\ \Im_{r,c} &\sim N(\mu, \sigma^2). \end{aligned} \tag{3}$$

A square block in Figure 2 represents a resolution cell. The total received complex scattered field of a resolution cell at position (r', c') is denoted as $\boldsymbol{A}_{r',c'}$, and the number of scatterers in the resolution cell is $N_{r',c'}$; thus

$$\boldsymbol{A}_{r',c'} = \Re_{r',c'} + j\Im_{r',c'} = \sum_{i=1}^{N_{r',c'}} \boldsymbol{a}_{r_i,c_i}, \tag{4}$$

where $\{(r_i, c_i), i = 1,2,\cdots, N_{r',c'}\}$ denotes the set of scatterers located within the resolution cell at position (r', c'). For an SAR image of size $L \times M$, the maximum number of scatterers per resolution is denoted as $N_{\max}$

$$N_{\max} = \max\{N_{r',c'}\}; 1 \le r' \le L, 1 \le c' \le M. \tag{5}$$

Denoting the scattered field of the ith scatterer in the resolution cell at position (r', c') as $\boldsymbol{A}_{(r',c',i)}$, then the total scattered field $\boldsymbol{A}_{r',c'}$ in the resolution cell is characterized in the $L \times M \times N_{\max}$ 3-D space as

$$\boldsymbol{A}_{r',c'} = \sum_{i=1}^{N_{r',c'}} \boldsymbol{A}_{r',c',i} \qquad (6)$$
$$1 \le r' \le L, 1 \le c' \le M, 1 \le i \le N_{\max},$$

where $\boldsymbol{A}_{r',c',i}$ is a nonzero value only when there is a scatterer at the position (r', c', i)

$$\boldsymbol{A}_{r',c',i} = \begin{cases} \boldsymbol{a}_{r_i,c_i}, & \text{if } 1 \le i \le N_{r',c'} \\ 0, & \text{if } N_{r',c'} < i \le N_{\max}, \end{cases} \qquad (7)$$

where $\boldsymbol{A}_{r',c',i} = 0$ indicates that there is no scatterer.

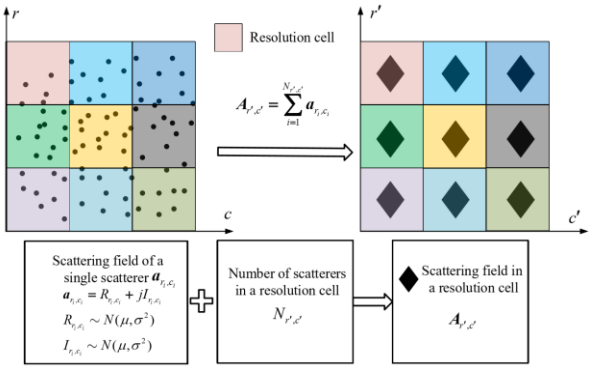

Figure 2. Gaussian coherent scatterer model

The texture information of an SAR image is caused by the spatial correlation of the distribution of underlying scatterers and the scatterer number. Both of them are treated as correlated random fields with a two-point correlation structure. The correlation coefficients of the underlying Gaussian scatterers and number of scatterers are determined by the correlation coefficient of the real-component and intensity SAR data according to the following correlation relationship:

$$\rho_{\Re\Re}(\tau) = \frac{E[min\{N(0), N(\tau)\}]}{\mu_N} E[\rho_{xx}(i,\tau)] \qquad (8)$$

$$\rho_{II}(\tau) = \frac{E[N_m N_m]\rho_{xx}^2(\tau) + \rho_{NN}(\tau)\sigma_N^2}{2\sigma_N^2 + \mu_N^2} \qquad (9)$$

where $\rho_{xx}(i,\tau)$, $\rho_{NN}(\tau)$, $\rho_{\Re\Re}(\tau)$ and $\rho_{II}(\tau)$ are correlation coefficients of underlying Gaussian scatterer, scatterer number, real-component and intensity SAR data, respectively. μ_N and σ_N^2 are the mean and variance of the scatterer number N, respectively. $N(0)$ denotes the scatterer number at current position while $N(\tau)$ is the scatterer number in the distance τ and $N_m = \min[N(0), N(\tau)]$.

The parameters of GGCS model [6] include 1) the distribution parameters of the underlying Gaussian scatterers and the number of scatterers, which determines the single-point probability distribution and 2) the convolution kernels of the underlying Gaussian scatterers and the number of scatterers, which determines the correlation structure. These parameters are all inferred from the statistical characteristics of a given SAR sample data. However, it is dependent on the preprocess step i.e. model selection and parameter estimation, which bring inconvenience and estimation deviation in practical applications. Therefore, a unified intelligent framework is needed for further physical analysis which brings the probabilistic graphical network below.

4 Probabilistic graphical network

Aiming to give an automated realization for the GGCS model, the probabilistic graphical network is proposed. The randomness and convolution operator of the GGCS model enlighten the proposal of the probabilistic graphical network shown in Figure 3. It represents the GGCS model by using multi-layer probabilistic convolutional neural networks.

The real component $\Re(x,y)$ and imaginary component $\Im(x,y)$ of the SAR image is modeled as:

$$\Re(x,y) = \sum_{k=1}^{M} \Re_k(x,y) = \sum_{k=1}^{M} G_k^{\Re}(x,y) \cdot b_k(x,y) \qquad (10)$$

$$\Im(x,y) = \sum_{k=1}^{M} \Im_k(x,y) = \sum_{k=1}^{M} G_k^{\Im}(x,y) \cdot b_k(x,y) \qquad (11)$$

where M is the number of channels, $G_k^{\Re}(x,y)$ and $G_k^{\Im}(x,y)$ are correlated Gaussian random filed with the correlation function $\rho_{g_i}(i = 1,2,\cdots,M)$, $b_k(x,y)$ is binary mask denoting the status of a scatterer which has:

$$b_k(x,y) = \begin{cases} 1, & \text{if there exists a scatterer} \\ 0, & \text{if there is no scatterer} \end{cases}. \qquad (12)$$

Different from the GGCS model, the channel of the number of scatterers is set as a constant M instead of a random variable by introducing the binary mask. This setting avoids the decorrelation effect caused by the variation of the number of scatterers. Then the amplitude image can be represented as:

$$A(x,y) = \sqrt{\Re^2(x,y) + \Im^2(x,y)}. \qquad (13)$$

The framework yields a directional graphical model [8] starting from the Gaussian random variables and binary random variables. The correlation property can be introduced by a convolution operation which can be realized using convolutional layer. The whole framework should be a trainable network which can obtain the parameters automatically by optimizing the error of the simulated and real SAR images. The primary correlated SAR clutter simulated results based on the probabilistic graphical network are shown in Figure 4 by setting Gaussian kernels. The probabilistic graphical network

shows its advantage on the parameter modeling and is potential for further intelligent realization of GGCS model which is useful for the deeply statistical analysis of SAR images.

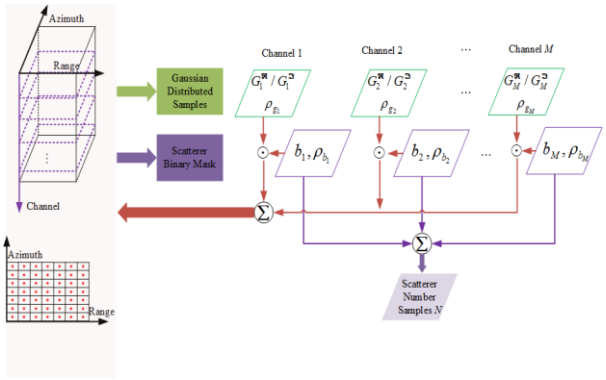

Figure 3. The framework of probabilistic graphical network

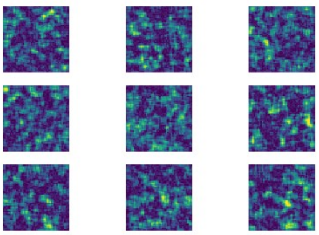

Figure 4. Simulated correlated clutter by probabilistic graphical network where Gaussian kernels is adopted

5 Conclusion

A physical perspective of correlated SAR clutter is analyzed in this paper. Several non-Rayleigh distributions models are re-analyzed based on the coherent scatterer model building on the physical scattering process. The physical analysis gives birth to the proposal of the GGCS model which is a physics-plausible generalized framework for existing several distributions. To enable automatic and intelligent realization of the GGCS model, the probabilistic graphical network is introduced for its strong learning ability. This paper focuses on the physical analysis of the SAR clutter which is critical for the interpretation of high-resolution SAR images.

6 Acknowledgements

This work was supported in part by the National Key Research and Development Program of China under Grant 2017YFB0502703 and in part by the Natural Science Foundation of China under Grant 61822107, Grant 61991422, and Grant 61571134.

7 References

1. C. Oliver and S. Quegan, “Understanding Synthetic Aperture Radar Images,” *Raleigh, USA: SciTech Publishing, Inc.*, 2004.

2. J. S. Lee and E. Pottier, “Polarimetric Radar Imaging: From Basics to Applications,” *Baton Rouge, United States.: CRC press-Taylor & Francis Group*, 2009.

3. G. Gui, "Statistical modeling of SAR images: a survey," *Sensors*, **10**, 1, 2010, pp. 775-795, doi:10.3390/s100100775.

4. G. Di Martino, A. Iodice, D. Riccio, and G. Ruello, “A physical approach for SAR speckle simulation: First results,” *Eur. J. Remote Sens.*, **46**, **1**, 2013, pp. 823–836, doi:10.5721/EuJRS20134649.

5. X. Deng, C. López-Martínez, and E. M. Varona, “A physical analysis of polarimetric SAR data statistical models,” *IEEE Trans. Geosci. Remote Sens.*, **54**, **5**, May 2016, pp. 3035–3048, doi: 10.1109/TGRS.2015.2510399.

6. D.-X. Yue, F. Xu, A. C. Frery, and Y.-Q. Jin, "A generalized Gaussian coherent scatterer mdoel for correlated SAR texture," *IEEE Trans. Geosci. Remote Sensing,* early access, 2019, doi: 10.1109/TGRS.2019.2958125.

7. E. Jakeman and P. N. Pusey, “A model for non-Rayleigh sea echo,” *IEEE Trans. Antennas Propag.*, **24**, 6, Nov. 1976, pp. 806–814, doi: 10.1109/TAP.1976.1141451.

8. D. Koller and N. Friedman, “Probabilistic graphical models: principles and techniques,” *Massachusetts Institute of Techniques*, 2009.

9. J. W. Goodman, “Speckle Phenomena in Optics: Theory and Applications,” *Greenwood Village, CO, USA: Ben Roberts and Company*, 2007.

10. T. Eltoft, “The Rician inverse Gaussian distribution: A new model for non-Rayleigh signal amplitude statistics,” *IEEE Trans. Image Process.*, **14**, 11, Nov. 2005, pp. 1722–1735, doi: 10.1109/TIP.2005.857281.

11. C. J. Oliver, “A model for non-Rayleigh scattering statistics,” *Opt. Acta, Int. J. Opt.*, **31**, 6, 1984, pp. 701–722, doi: 10.1080/713821561.

12. A. C. Frery, H.-J. Müller, C. C. F. Yanasse, and S. J. S. Sant’Anna, “A model for extremely heterogeneous clutter,” *IEEE Trans. Geosci. Remote Sens.*, **35**, 3, May 1997, pp. 648–659, doi: 10.1109/36.581981.

13. Y. Delignon and W. Pieczynski, “Modeling non-Rayleigh speckle distribution in SAR images,” *IEEE Trans. Geosci. Remote Sens.*, **40**, 6, Jun. 2002, pp. 1430–1435, doi:10.1109/TGRS.2002.800234.